



A model for the effect of pressure gradient on turbulent axisymmetric wakes

Sina Shamsoddin¹ and Fernando Porté-Agel^{1,†}

¹École Polytechnique Fédérale de Lausanne (EPFL), Wind Engineering and Renewable Energy Laboratory (WIRE), EPFL-ENAC-III-E-WIRE, CH-1015 Lausanne, Switzerland

(Received 11 October 2017; revised 22 November 2017; accepted 23 November 2017; first published online 4 January 2018)

Turbulent axisymmetric wakes under pressure gradient have received little attention in the literature, in spite of their fundamental and practical importance, for example, in the case of wind turbine wakes over topography. In this paper, we develop an analytical framework to analyse turbulent axisymmetric wakes under different pressure gradient conditions. Specifically, we develop a model to predict how an arbitrary imposed pressure gradient perturbs the evolution of the zero-pressure-gradient wake. The starting point of the model is the basic mean conservation of the streamwise momentum equation. We take advantage of the self-similarity of the wake velocity deficit and the assumption that the ratio of the maximum velocity deficit to the wake width is independent of the pressure gradient; such an assumption is supported experimentally for planar wakes, and numerically for axisymmetric wakes in this study. Furthermore, an asymptotic solution for the problem is also derived. The problem is considered for both an axisymmetric strain and a planar strain. The inputs to the model are the imposed pressure gradient and the wake width in the zero-pressure-gradient case. To validate the model results, a set of large-eddy simulations (LES) are performed. Comparing the evolution of the maximum velocity deficit and the wake width, the model results and the LES data show good agreement. Similarly to planar wakes, it is observed that the axisymmetric wake recovers faster in the favourable pressure gradient compared with the adverse one.

Key words: general fluid mechanics, turbulent flows, wakes

1. Introduction

The problem of turbulent axisymmetric wakes under pressure gradient is interesting, and its study is useful; first, because it can be regarded as a classical fundamental fluid mechanics problem, and, second, because such a phenomenon can have engineering

† Email address for correspondence: fernando.porte-agel@epfl.ch

implications. One example that is worthy of attention is the design of wind farms sited on topography. The axisymmetric wind turbine wakes are subjected to non-zero pressure gradients, which are caused by variations in the underlying terrain elevation. This changes the wake recovery characteristics of the wind turbines with respect to the flat terrain case, and, in turn, can affect the design of the optimum layout of the wind farm.

In spite of its importance, few studies have been carried out on this subject. In their analytical study on wakes in complex flows, Hunt & Eames (2002), among other things, derived the solution for the mean velocity for a laminar axisymmetric wake under a specific strain caused by an external flow. Magnaudet, Rivero & Fabre (1995) and Bagchi & Balachandar (2002) performed numerical simulations of flow past a sphere (rigid and bubble-like) that was subjected to strain (planar and axisymmetric). The focus of their studies was more on the direct impact of the flow on the sphere (e.g. forces, separation, etc.) rather than the evolution of the wake itself. In contrast to turbulent axisymmetric wakes, some interesting research has already been performed for the planar case using numerical (Rogers 2002) and experimental (Liu, Thomas & Nelson 2002; Thomas & Liu 2004) approaches, supported also by concurrent analytical (Shamsoddin & Porté-Agel 2017*b*) developments. Based on these studies, it is known that favourable pressure gradients (accelerating base flows) lead to a faster recovery of the wake.

As mentioned in the conclusion of Shamsoddin & Porté-Agel (2017*b*), turbulent axisymmetric wakes ought to be studied under the influence of imposed pressure gradients, especially because of the arising of such scenarios in the case of wind turbine wakes over topography. In the present paper, we aim to accomplish this objective by proposing an analytical framework to analyse such wakes and eventually by developing a model to predict how an arbitrary imposed non-zero pressure gradient alters the evolution of a turbulent axisymmetric wake under zero pressure gradient. In addition, we provide large-eddy simulation (LES) results related to such wakes, against which we can test our model. To the best knowledge of the authors, no study (experimental, numerical or analytical) on this topic (turbulent axisymmetric wakes under different imposed pressure gradients) is available in the literature. Therefore, this paper can provide useful insight (by presenting both a theoretical framework and an LES dataset) related to this subject.

This article is ordered in the following manner. In § 2, the problem is defined and the model is derived with all of its variants. In § 3, the numerical experiments, which are performed for the purpose of validation of the model, are described and their results are compared with the predictions of the model. Finally, § 4 concludes the paper.

2. Analytical model for axisymmetric wakes under pressure gradient

2.1. Problem formulation

The mean velocity deficit profiles of turbulent axisymmetric wakes are known to be self-similar and to have a Gaussian shape function (Pope 2000),

$$\frac{U_b(x) - \bar{u}(x, r)}{U_b(x)} \equiv C(x)e^{-(r^2/2\delta^2)}, \quad (2.1)$$

where x is the streamwise direction, r is the radial direction from the wake centre, $\bar{u}(x, r)$ is the velocity (hereafter, by velocity, we imply the mean streamwise velocity,

A model for the effect of pressure gradient on turbulent axisymmetric wakes

unless otherwise stated) of the wake flow, $U_b(x)$ is the velocity of the base flow, $C(x)$ is a function determining the maximum velocity deficit at each x -position and $\delta(x)$ is the wake width.

Here, we assume that the axisymmetric wake retains its Gaussian shape under non-zero pressure gradients. This assumption will be verified later in this paper (§ 3). It is noteworthy to mention that it has already been shown that for a turbulent planar wake, this assumption is valid (Liu *et al.* 2002; Rogers 2002; Shamsoddin & Porté-Agel 2017b).

The imposed pressure gradient is manifested in the above formulation in the function $U_b(x)$. For an accelerating base flow ($dU_b/dx > 0$), we have the so-called favourable pressure gradient (FPG), and for a decelerating base flow ($dU_b/dx < 0$), we have the so-called adverse pressure gradient (APG). Obviously, for the zero-pressure-gradient (ZPG) case, $U_b(x) = U_{b0} = \text{const.}$

Our objective in this section is to solve the following problem: for a given ZPG wake (for which we know the wake width evolution), how is the mean velocity field of the wake (i.e. $C(x)$ and $\delta(x)$) changed after imposing an arbitrary pressure gradient?

2.2. Model derivation

The mean conservation of momentum equation in the x -direction for a turbulent axisymmetric wake can be written as

$$\frac{\partial \bar{u}(U_b - \bar{u})}{\partial x} + \frac{\partial \bar{v}(U_b - \bar{u})}{\partial y} + \frac{\partial \bar{w}(U_b - \bar{u})}{\partial z} = -\frac{dU_b}{dx}(U_b - \bar{u}) + \frac{\partial \overline{u'v'}}{\partial y} + \frac{\partial \overline{u'w'}}{\partial z}, \quad (2.2)$$

where u , v and w are the streamwise (x), lateral (y) and vertical (z) components of the velocity, the overbar indicates a mean quantity and the prime shows the fluctuation quantities (e.g. $u' = u - \bar{u}$). In deriving this equation, the continuity equation is used, the viscous and $\partial \overline{u^2}/\partial x$ terms are neglected, and the mean pressure gradient term, $-(1/\rho)\partial \bar{p}/\partial x$, is replaced by $U_b(dU_b/dx)$. For intermediate steps, through which this equation is obtained, the interested reader is referred to Shamsoddin & Porté-Agel (2017b).

After integrating in the x -normal plane, we obtain the integral form of the x -momentum equation,

$$\frac{d}{dx} \int_0^\infty \bar{u}(U_b - \bar{u})(2\pi r dr) + \int_0^\infty \frac{dU_b}{dx}(U_b - \bar{u})(2\pi r dr) = 0. \quad (2.3)$$

It should be noted that, as $(U_b - \bar{u})$, $\overline{u'v'}$ and $\overline{u'w'}$ all vanish far from the wake centre (in a given x -normal plane), the integrals of the last two terms on both sides of (2.2) are zero. Here, we assume that the strain that causes the pressure gradient is also axisymmetric, and therefore the wake retains its axisymmetry after imposing the pressure gradient (for the case of a planar strain, see § 2.4). Thus, we can directly substitute (2.1) into (2.3) and use $\int_0^\infty \exp[-r^2/(2\delta^2)](2\pi r dr) = 2\pi\delta^2$ to obtain

$$\frac{d}{dx} \left[2\pi U_b^2(x)\delta^2(x) \left(C(x) - \frac{C^2(x)}{2} \right) \right] + \pi \frac{dU_b^2}{dx} \delta^2(x) C(x) = 0. \quad (2.4)$$

As can be seen, we are left with a nonlinear ordinary differential equation (ODE). We first show the solution of the equation for the ZPG case, because it proves to

be helpful later. In fact, in the ZPG case, (2.4) reduces to an algebraic equation (the second term vanishes), whose solution has already been obtained by Bastankhah & Porté-Agel (2014),

$$C_0(x) = 1 - \sqrt{1 - \frac{C_D}{8 \left(\frac{\delta_0(x)}{D}\right)^2}} \quad (x \geq x_i), \tag{2.5}$$

where the subscript 0 indicates a quantity in the ZPG case, D is the diameter of the wake-generating object and C_D is the drag coefficient of the object (or in the case of a power-generating device, the thrust coefficient). The condition ($x \geq x_i$) is only to make sure that the expression under the square root always remains non-negative.

Now, we focus on the ODE of (2.4). In this ODE, we have one equation and two unknowns (C and δ). Therefore, we need another equation to close the problem. For this purpose, following Shamsoddin & Porté-Agel (2017b), we use the invariance of the ratio $\lambda(x) \equiv U_d(x)/\delta(x)$ under pressure gradient changes, where $U_d(x) \equiv C(x)U_b(x)$ is the maximum velocity deficit at a given streamwise position. This invariance has been shown experimentally (Liu *et al.* 2002; Thomas & Liu 2004) and has been used to develop a model for the case of planar wakes by Shamsoddin & Porté-Agel (2017b). For the case of axisymmetric wakes, we will reaffirm the validity of this assumption based on LES data in § 3. Hence, because λ is insensitive to pressure gradient and thus U_b , we have

$$\lambda(x) = \lambda_0(x) = \frac{U_{b0}C_0(x)}{\delta_0(x)}. \tag{2.6}$$

Consequently, δ can be expressed as

$$\delta(x) = \frac{U_b(x)}{\lambda_0(x)}C(x). \tag{2.7}$$

Now, substituting (2.7) into (2.4), the final ODE for $C(x)$ is obtained,

$$\frac{dC(x)}{dx} = \frac{-1}{\left(\frac{U_b^4}{\lambda_0^2}\right) (3C^2 - 2C^3)} \left[\frac{1}{4} \frac{dU_b^4}{dx} \frac{C^3}{\lambda_0^2} + \left(C^3 - \frac{C^4}{2}\right) \frac{d}{dx} \left(\frac{U_b^4}{\lambda_0^2}\right) \right], \tag{2.8}$$

with the boundary condition

$$C(x_i) = C_0(x_i). \tag{2.9}$$

Equation (2.8) is a nonlinear ODE in the explicit form of $dC(x)/dx = f(U_b, \lambda_0, C(x))$. This ODE can be solved easily and rapidly with common commercial ODE solvers. Thus, with (2.8) and (2.9), our objective, which was the solution of the problem defined in § 2.1, is accomplished.

2.3. Asymptotic solution of the problem

Since $\bar{u} \rightarrow U_b$ far downstream of the wake-generating object, we have $C^2(x) \ll C(x)$ for sufficiently large x (at least for the FPG and ZPG cases) (Shamsoddin & Porté-Agel 2017b). Therefore, neglect of the term involving $C^2(x)$ in (2.4) leads to the following linear ODE:

$$\frac{d}{dx} \left[2\pi U_b^2(x) \delta^2(x) \tilde{C}(x) \right] + \pi \frac{dU_b^2}{dx} \delta^2(x) \tilde{C}(x) = 0, \quad (2.10)$$

where \tilde{C} is the asymptotic solution of C . The above equation is exactly equivalent to the following:

$$2\pi \frac{1}{U_b} \frac{d}{dx} \left[\delta^2(x) \tilde{C}(x) U_b^3 \right] = 0. \quad (2.11)$$

Using the readily obtainable asymptotic ZPG solution for \tilde{C}_0 from (2.4) (i.e. $\tilde{C}_0 = D^2 C_D / (16\delta_0^2)$) to find the correct constant of integration, the solution to (2.11) can be found as

$$\tilde{C}(x) = \frac{1}{16} \frac{C_D}{\left(\frac{\delta(x)}{D}\right)^2} \left(\frac{U_{b0}}{U_b(x)}\right)^3, \quad (2.12)$$

which by employing (2.6)–(2.7) can be further simplified to

$$\tilde{C}(x) = \tilde{C}_0 \left(\frac{U_{b0}}{U_b(x)}\right)^{5/3}. \quad (2.13)$$

It is noteworthy that for the planar case the exponent of (U_{b0}/U_b) was found to be 2 (Shamsoddin & Porté-Agel 2017b), whereas for the axisymmetric case this exponent is 5/3. Furthermore, $\tilde{C}_0(x)$ can be shown to be the second-order Taylor expansion of the full solution of $C_0(x)$, i.e. (2.5), in terms of δ_0^{-1} .

2.4. Axisymmetric wakes and planar strain

In the above derivations, we had assumed an axisymmetric strain and, consequently, that the wake retains its axisymmetry (e.g. when a wake passes through a circular nozzle/diffuser). This assumption provides a perfect analogy to the case of a planar wake under a planar strain (e.g. Liu *et al.* 2002; Thomas & Liu 2004; Shamsoddin & Porté-Agel 2017b). In this subsection, we are interested in studying the case of an axisymmetric wake that undergoes an imposed pressure gradient that is a result of a planar strain (e.g. when passing through a planar nozzle/diffuser). This case is interesting because of its practical use, in particular, for the case of wind turbine wakes flowing over topography: in this case the topography generates a planar strain on the axisymmetric wake of a wind turbine rotor.

Without losing generality, we consider the planar strain to be in the z -direction. In this case (unlike the axisymmetric strain case), the wake widths in the y - and z -directions are not necessarily equal. Therefore, following Bastankhah & Porté-Agel

(2016), we assume that the velocity deficit profile of the wake has the following general shape:

$$\frac{U_b(x) - \bar{u}(x, y, z)}{U_b(x)} \equiv C(x) \exp \left[- \left(\frac{y^2}{2\delta_y^2} + \frac{z^2}{2\delta_z^2} \right) \right], \quad (2.14)$$

where δ_y and δ_z are the wake widths in the y - and z -directions. In the case of $\delta_y = \delta_z$, the above equation reduces to (2.1) (as in Vermeulen, Bultjes & Dekker 1979; Jensen 1983; Bastankhah & Porté-Agel 2014). We have $\int_{-\infty}^{\infty} \int_{-\infty}^{\infty} \exp[-(y^2/(2\delta_y^2) + z^2/(2\delta_z^2))] dydz = 2\pi\delta_y\delta_z$, and this paves the way to define an equivalent wake width δ_{eq} as the geometric mean of δ_y and δ_z ,

$$\delta_{eq} = \sqrt{\delta_y\delta_z}. \quad (2.15)$$

Now, if we substitute (2.14) into (2.3), and follow the same procedure as in §§ 2.2 and 2.3, we obtain exactly the same equations, with the only difference being that δ_{eq} replaces δ in all of those equations.

In fact, in the case of planar strain, we solve our problem for $C(x)$ and $\delta_{eq}(x)$. In order to further obtain δ_y and δ_z individually, we require more information about the geometry and history of the flow and strain, which is beyond the scope of the framework of the current model. However, being able to predict $C(x)$ and δ_{eq} still enables us to obtain a great deal of information about the flow which can be useful in many practical applications.

3. Validation of the model

3.1. The numerical experiment

To validate the model, we compare its results with results from the LES of axisymmetric wakes in three specific FPG, ZPG and APG cases. The numerical experiments are performed in an ideal spanwise-periodic channel with rectangular cross-section. To create the desired non-zero pressure gradient, the walls of the channel are curved so that its cross-sectional area varies in the streamwise direction. The wake itself is generated with an actuator disk of diameter D and drag (or thrust) coefficient $C_D = 0.8$. As can be seen in figure 1, three different geometries of the channel wall are used respectively for the FPG, ZPG and APG cases: (i) convex walls, which create a contraction and consequently flow acceleration ($dU_b/dx > 0$) up to the channel throat, (ii) straight walls, which create neither acceleration nor deceleration ($dU_b/dx = 0$) along the channel, and (iii) concave walls, which create an expansion and consequently flow deceleration ($dU_b/dx < 0$) up to the channel throat. The upper and lower walls are symmetric with respect to the centre plane of the channel, and the surface equation of the lower wall has the following general cosine form:

$$Z_s(x) = \begin{cases} \frac{1}{2}h \left[1 + \cos \left[\frac{\pi}{2L_1}(x - x_{th}) \right] \right], & -2L_1 \leq x - x_{th} < 0, \\ \frac{1}{2}h \left[1 + \cos \left[\frac{\pi}{2L_2}(x - x_{th}) \right] \right], & 0 \leq x - x_{th} < 2L_2, \\ 0, & \text{otherwise,} \end{cases} \quad (3.1)$$

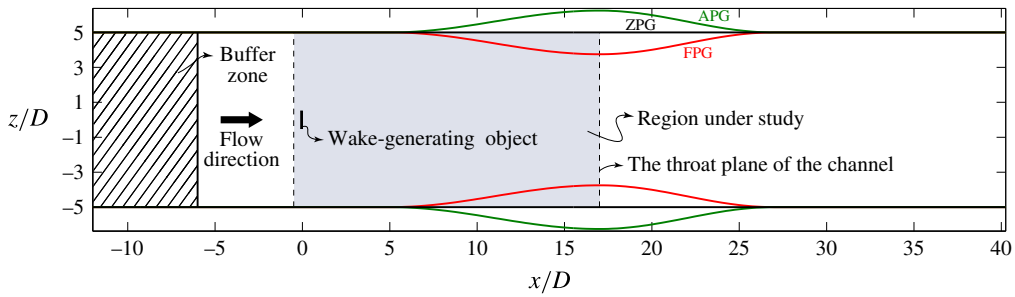


FIGURE 1. The domain of the simulations.

where Z_s is the height of the wall with respect to the straight wall of the ZPG case, the origin of x (as shown in figure 1) is the position of the wake-generating disk, $x_{th} = 17D$ is the position of the channel throat, h is the maximum height of the wall (occurring at the throat), which has values of $1.25D$, 0 and $-1.25D$ for the FPG, ZPG and APG cases respectively, and $L_1 = 6D$ and $L_2 = 5D$ are the half-lengths of the cosine functions for the sections upstream and downstream of the throat respectively. In each case, the region in which we are interested for our study is the region downstream of the disk up until the throat of the channel. This region is shown by the shaded area in figure 1.

For the sake of conciseness and without affecting the purpose of the paper, we do not include the details of the LES framework here, to avoid repetition of what is already available in the literature. The governing equations (the momentum and continuity equations), general numerics and subgrid-scale model (the Lagrangian scale-dependent dynamic model) are described in Porté-Agel, Meneveau & Parlange (2000) and Stoll & Porté-Agel (2006). To model the wake-generating disk, we use the standard actuator disk model (Wu & Porté-Agel 2011). To resolve the curved wall of the channel, a coordinate transformation technique is employed, whose details can be found in Shamsoddin & Porté-Agel (2017a) (with the slight difference that in that study the domain comprised the half-channel). The boundary conditions in the horizontal directions are mathematically periodic. For the upper and lower channel walls, the instantaneous surface shear stress is calculated using the Monin–Obukhov similarity theory (which for the neutral case of this study simply reduces to the log law). To overcome the streamwise periodicity and to have a prescribed inflow to the domain, a buffer zone technique is used to feed an inflow field that is generated offline by performing a precursory simulation in a periodic straight channel (Shamsoddin & Porté-Agel 2017a). It should be noted that the turbulence intensity of the incoming flow at the centre of the channel (defined as the standard deviation of the streamwise velocity divided by U_{b0}) is 0.03 for all cases.

The streamwise (x), spanwise (y) and vertical (z) lengths of the computational domain are $52.5D$, $8.75D$ and $10D$ respectively. The numbers of grid points in the x -, y - and z -directions are 210, 60 and 122. Regarding the accuracy and validations of the framework, it should be noted that the validation of the actuator disk model was carried out in Wu & Porté-Agel (2011) and the validation of the coordinate transformation technique was carried out in Wan, Porté-Agel & Stoll (2007). On top of these, the combined application of the actuator disk and coordinate transformation methods was validated in Shamsoddin & Porté-Agel (2017a). The chosen resolution of the grid is well within the range that has been previously shown to result in

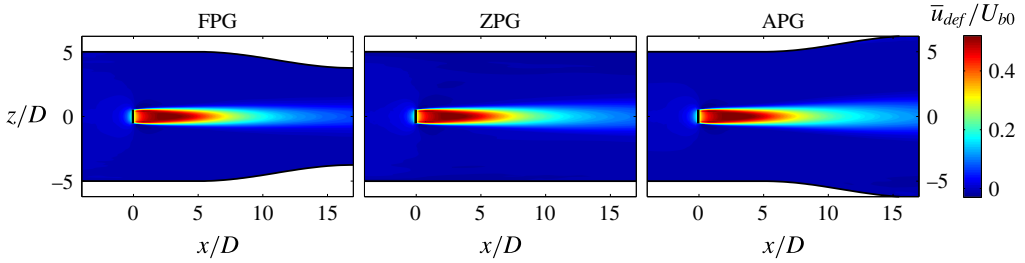


FIGURE 2. Contours of the normalized velocity deficit in the FPG, ZPG and APG cases.

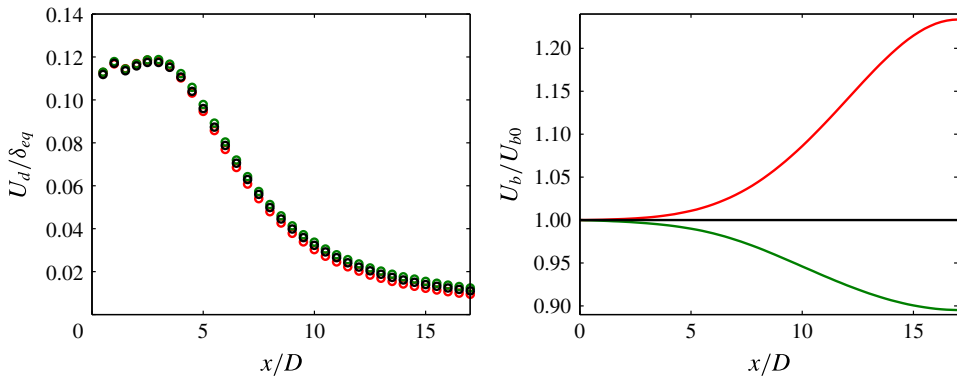


FIGURE 3. (a) Evolution of $\lambda(x)$ as a function of streamwise distance and (b) base flow velocity $U_b(x)$ for the FPG (red), ZPG (black) and APG (green) cases.

grid-independent results for the cases of application of the coordinate transformation (see Wan *et al.* 2007, § 3) and flow through actuator disks (see Wu & Porté-Agel 2011, § 4; Wu & Porté-Agel 2013, § 4.1), and the case of the combined application of the coordinate transformation and actuator disks (Shamsoddin & Porté-Agel 2017a).

3.2. Results and comparison

For each case, we perform two simulations: one without the presence of the disk, which serves as the base flow field, and one with the presence of the disk. To isolate the turbine wake, and in accordance with § 2.1, we define the velocity deficit as follows:

$$\bar{u}_{def}(x, y, z) = \bar{u}_{nw}(x, y, z) - \bar{u}_w(x, y, z), \quad (3.2)$$

where the subscripts *w* and *nw* indicate wake and no-wake cases respectively. In other words, to obtain the velocity deficit at a given point, we subtract the velocity of that point in the wake case from the velocity of the same point in the no-wake case. Figure 2 shows the contours of \bar{u}_{def} in all three cases. The larger width and slower recovery of the APG wake compared with the FPG one is clear in this figure. Before applying the developed model of § 2, we need to extract $U_b(x) = \bar{u}_{nw}(x, 0, 0)$, which is an input to the model, and also to verify the assumption of (2.6). Figure 3 shows these two pieces of information. As can be seen, $\lambda(x) = U_d(x)/\delta(x)$ is almost independent of pressure gradient for these three cases. It is also noteworthy that the blockage ratio

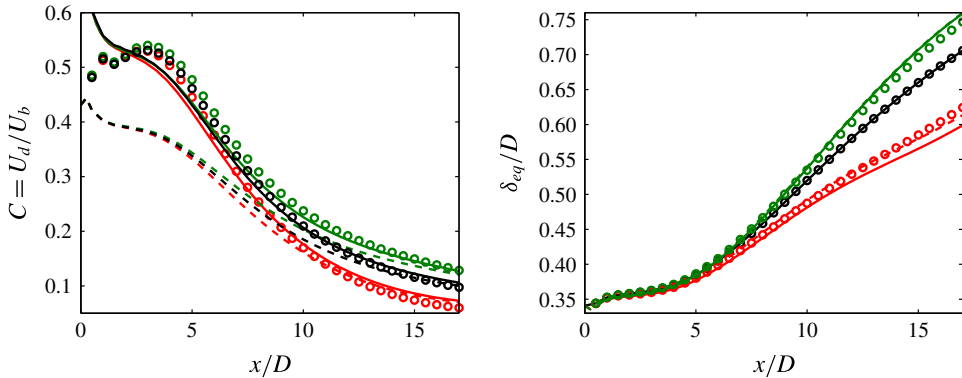


FIGURE 4. Normalized maximum velocity deficit (a) and wake width (b) as a function of the streamwise distance for the ZPG (black), FPG (red) and APG (green) cases. The circles indicate LES results, the solid lines are the full solution obtained from (2.8) and the dashed lines are the asymptotic solution of (2.13).

of the turbine in the channel is 0.009, which can safely be considered as negligible (Segalini & Inghels 2014).

Now we are ready to implement our proposed model in the aforementioned cases, to see how it predicts the effect of pressure gradient on the wake. Figure 4 shows the comparison of the results of the LES and the model for the streamwise evolution of $C(x)$ and δ_{eq} . It can be observed that the model predictions agree well with the LES results. In the figure, in addition to the full solution of the ODE (2.8), the asymptotic solutions, resulting from (2.13), are also shown. It should be noted that all ODEs in this paper are solved with the ‘ode45’ routine of MATLAB, which uses an explicit Runge–Kutta (4,5) algorithm, namely the Dormand–Prince method. The black curve in figure 4(b), i.e. $\delta_0(x)$, is the input of the model, together with the $U_b(x)$, which is shown in figure 3(b). Thus, the model results shown here are independently reproducible by the interested reader simply by using the information provided in this paper. Moreover, figure 5 shows a comparison of the normalized velocity deficit profiles in the z - and y -directions obtained from the LES and the model for both the FPG and the APG cases. It can be observed that the model can reproduce the profiles with a good accuracy.

4. Concluding remarks

We have developed an analytical model that enables us to predict the effect of an imposed pressure gradient on the evolution of turbulent axisymmetric wakes. In particular, the model predicts how the evolution of the maximum velocity deficit and width of the wake is altered with respect to the ZPG case by the imposed pressure gradient. The model uses cross-stream integration of the basic mean momentum conservation equation, the self-similarity of the wake and the assumption that the ratio of the maximum velocity deficit to the wake width is invariant under pressure gradient changes. The validity of this assumption has been shown experimentally for planar wakes (Liu *et al.* 2002) and we have reaffirmed it here for axisymmetric wakes with our LES. An asymptotic solution of the problem is also provided. The problem is considered for both an axisymmetric strain and a planar one. The inputs to the model are the imposed pressure gradient and the wake width in the ZPG case.

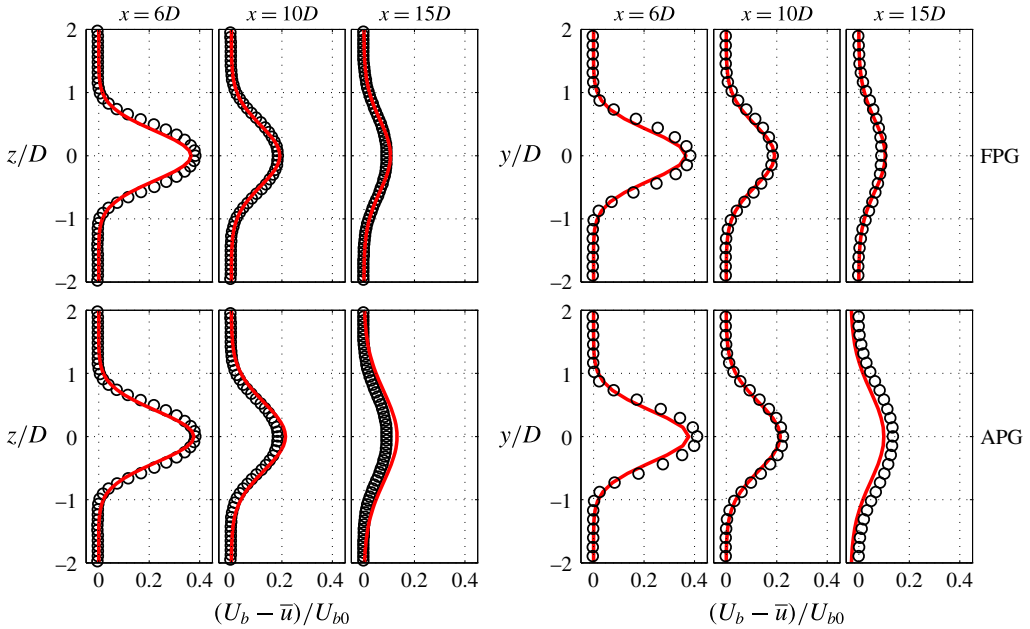


FIGURE 5. Normalized velocity deficit profiles at different streamwise positions. The circles show LES results and the red lines show the model predictions.

For the purposes of validation of the model, a set of numerical experiments, using LES, were performed. After comparing the maximum velocity deficit and wake width predicted by the model with those of the LES, a good agreement was observed.

As mentioned in the introduction, one pertinent practical situation where turbulent axisymmetric wakes under pressure gradient conditions emerge in the real world is the case of wind turbine wakes over topography. However, it is important to note that for such cases, in addition to the pressure gradient effects, there is also the effect of streamline curvature. One particular value of the present work is that it isolates the effect of pressure gradient, as it considers a wake whose centreline is straight (no streamline curvature). In other words, we have decoupled the effect of pressure gradient from that of streamline curvature. That being said, the effect of streamline curvature also has to be taken into account for a proper understanding of the problem of wakes over topography. This issue will be addressed in our future research.

Acknowledgements

This research was supported by EOS (Energie Ouest Suisse) Holding, the Swiss Federal Office of Energy (Grant SI/501337-01), the Swiss National Science Foundation (grant 200021_172538) and the Swiss Innovation and Technology Committee (CTI) within the context of the Swiss Competence Center for Energy Research ‘FURIES: Future Swiss Electrical Infrastructure’. Computing resources were provided by the Swiss National Supercomputing Centre (CSCS) under Project ID s706.

References

- BAGCHI, P. & BALACHANDAR, S. 2002 Steady planar straining flow past a rigid sphere at moderate Reynolds number. *J. Fluid Mech.* **466**, 365–407.
- BASTANKHAH, M. & PORTÉ-AGEL, F. 2014 A new analytical model for wind-turbine wakes. *J. Renew. Energy* **70**, 116–123; special issue on aerodynamics of offshore wind energy systems and wakes.
- BASTANKHAH, M. & PORTÉ-AGEL, F. 2016 Experimental and theoretical study of wind-turbine wakes in yawed conditions. *J. Fluid Mech.* **806**, 506–541.
- HUNT, J. C. R. & EAMES, I. 2002 The disappearance of laminar and turbulent wakes in complex flows. *J. Fluid Mech.* **457**, 111–132.
- JENSEN, N. O. 1983 A note on wind generator interaction. *Tech. Rep.* Risø-M-2411. Risø National Laboratory, Roskilde.
- LIU, X., THOMAS, F. O. & NELSON, R. C. 2002 An experimental investigation of the planar turbulent wake in constant pressure gradient. *Phys. Fluids* **14** (8), 2817–2838.
- MAGNAUDET, J., RIVERO, M. & FABRE, J. 1995 Accelerated flows past a rigid sphere or a spherical bubble. Part 1. steady straining flow. *J. Fluid Mech.* **284**, 97–135.
- POPE, S. B. 2000 *Turbulent Flows*. Cambridge University Press.
- PORTÉ-AGEL, F., MENEVEAU, C. & PARLANGE, M. B. 2000 A scale-dependent dynamic model for large-eddy simulation: application to a neutral atmospheric boundary layer. *J. Fluid Mech.* **415**, 261–284.
- ROGERS, M. M. 2002 The evolution of strained turbulent plane wakes. *J. Fluid Mech.* **463**, 53–120.
- SEGALINI, A. & INGHELIS, P. 2014 Confinement effects in wind-turbine and propeller measurements. *J. Fluid Mech.* **756**, 110–129.
- SHAMSODDIN, S. & PORTÉ-AGEL, F. 2017a Large-eddy simulation of atmospheric boundary-layer flow through a wind farm sited on topography. *Boundary-Layer Meteorol.* **163** (1), 1–17.
- SHAMSODDIN, S. & PORTÉ-AGEL, F. 2017b Turbulent planar wakes under pressure gradient conditions. *J. Fluid Mech.* **830**.
- STOLL, R. & PORTÉ-AGEL, F. 2006 Dynamic subgrid-scale models for momentum and scalar fluxes in large-eddy simulation of neutrally stratified atmospheric boundary layers over heterogeneous terrain. *Water Resour. Res.* **42**, W01409.
- THOMAS, F. O. & LIU, X. 2004 An experimental investigation of symmetric and asymmetric turbulent wake development in pressure gradient. *Phys. Fluids* **16** (5), 1725–1745.
- VERMEULEN, P. E. J., BUILTJES, P., DEKKER, J. & LAMMERTS VAN BUEREN, G. 1979 An experimental study of the wake behind a full scale vertical-axis wind turbine. *Tech. Rep.* 79-06118. TNO.
- WAN, F., PORTÉ-AGEL, F. & STOLL, R. 2007 Evaluation of dynamic subgrid-scale models in large-eddy simulations of neutral turbulent flow over a two-dimensional sinusoidal hill. *Atmos. Environ.* **41** (13), 2719–2728.
- WU, Y. T. & PORTÉ-AGEL, F. 2011 Large-eddy simulation of wind-turbine wakes: evaluation of turbine parametrisations. *Boundary-Layer Meteorol.* **138** (3), 345–366.
- WU, Y. T. & PORTÉ-AGEL, F. 2013 Simulation of turbulent flow inside and above wind farms: model validation and layout effects. *Boundary-Layer Meteorol.* **146** (2), 181–205.